

# Robust Two-Qubit Gates for Donors in Silicon Controlled by Hyperfine Interactions

Rachpon Kalra,<sup>1</sup> Arne Laucht,<sup>1</sup> Charles D. Hill,<sup>2</sup> and Andrea Morello<sup>1\*</sup>

<sup>1</sup>*Centre for Quantum Computation and Communication Technology,  
School of Electrical Engineering & Telecommunications, University of New South Wales,  
Sydney, New South Wales 2052, Australia*

<sup>2</sup>*Centre for Quantum Computation and Communication Technology, School of Physics,  
University of Melbourne, Melbourne, Victoria 3010, Australia*

(Received 11 December 2013; revised manuscript received 13 February 2014; published 6 June 2014)

We present two strategies for performing two-qubit operations on the electron spins of an exchange-coupled pair of donors in silicon, using the ability to set the donor nuclear spins in arbitrary states. The effective magnetic detuning of the two electron qubits is provided by the hyperfine interaction when the two nuclei are prepared in opposite spin states. This can be exploited to switch SWAP operations on and off with modest tuning of the electron exchange interaction. Furthermore, the hyperfine detuning enables high-fidelity conditional rotation gates based on selective resonant excitation. The latter requires no dynamic tuning of the exchange interaction at all and offers a very attractive scheme to implement two-qubit logic gates under realistic experimental conditions.

DOI: [10.1103/PhysRevX.4.021044](https://doi.org/10.1103/PhysRevX.4.021044)

Subject Areas: Nanophysics, Quantum Physics,  
Quantum Information

## I. INTRODUCTION

The electron spin of a donor atom in silicon represents a natural, highly coherent quantum bit. It is bound to a well-defined confining potential and is hosted by the most important material in modern technology. The recent demonstrations of high-fidelity single-shot readout [1] and control of both the electron [2] and the nuclear [3] spins of a <sup>31</sup>P donor in a silicon nanostructure have added tremendous momentum to this quantum computer architecture [4,5]. The next step towards constructing a universal set of quantum gates is to demonstrate two-qubit logic operations [6]. This has been accomplished in several architectures, including those of photonic qubits [7], superconducting circuits [8], qubits defined in quantum dots [9,10], atoms in electromagnetic traps [11], and nitrogen-vacancy centers in diamond [12]. While several proposals for the implementation of a two-qubit gate with donor electrons exist [13–15], they pose very challenging demands on the tunability of the spin exchange interaction  $J$ , which is assumed to be switchable from around 0 to  $> 1$  GHz. It is also predicted that  $J$  can vary strongly upon displacing a donor by even a single lattice site [16,17], thus requiring true atomic precision in the placement of the donors. These considerations have contributed

to creating some skepticism on the viability of donor-spin qubits for large quantum computer architectures.

Here, we propose two implementations of two-qubit gates that overcome these challenges. Both of these gates, when combined with previously demonstrated single-qubit operations [2], are universal for quantum computing. Our proposals are based on exploiting the hyperfine interaction  $A$  with the donor nuclear spins, and the ability to control the nuclear spin state. High-fidelity control and readout of a single <sup>31</sup>P nuclear spin has been established experimentally [3], validating our main assumption. It was also found that a nuclear spin prepared in an eigenstate maintains its state for several minutes [3]. The core of the idea is to prepare the nuclei in opposite spin states so that the hyperfine coupling provides a substantial difference in the local magnetic field experienced by the electrons. In a many-qubit quantum processor, it will be possible to prepare the state of individual nuclear spins by selectively ionizing the donors whose nucleus we wish to control, since an ionized donor has a resonance frequency that differs from the two nuclear resonances of a neutral donor by several MHz [3]. Magnetically detuning the energies of electron-spin qubits has been proposed [18] and implemented in several ways, including the fabrication of a micromagnet adjacent to the qubits [19], introducing an inequivalence in  $g$  factors [20], or dynamically polarizing the background nuclear spin bath [21]. In comparison, the initialization of the two nuclei in the two-donor system presents an extremely compact, consistent, and easily switchable source of magnetic detuning. It also avoids additional decoherence channels that can arise from the transverse component of an external magnetic-field gradient [22]. Importantly, both our

\*a.morello@unsw.edu.au

Published by the American Physical Society under the terms of the *Creative Commons Attribution 3.0 License*. Further distribution of this work must maintain attribution to the author(s) and the published article's title, journal citation, and DOI.

proposals rely upon weak exchange coupling  $J$ , comparable to or smaller than the hyperfine coupling  $A = 117$  MHz. This has the crucial advantage of suppressing a deleterious channel for triplet-singlet relaxation, predicted by Borhani and Hu [23] and observed by Dehollain *et al.* [24] when  $J \gg A$ .

In the first proposal, we focus on using the hyperfine interaction to switch the amplitude of exchange oscillations to perform a  $\sqrt{\text{SWAP}}$  gate, a rotation of angle  $\pi/2$  around the  $J$ -axis of the  $\mathcal{S} - \mathcal{T}_0$  Bloch sphere. This requires a reasonable 2-orders-of-magnitude control of  $J$ , which could be achieved with an easily fabricable device design. The second two-donor gate is a prototypical implementation of a conditional rotation (CROT), as demonstrated for superconducting qubits [8] and spin qubits in diamond [25]. This is the resonant rotation of one qubit conditional upon the state of the other. We show that high-fidelity entangling two-qubit gates can be performed between donor pairs. Dynamic control of the exchange coupling is not required at all in this case, and high-fidelity gates can be achieved for a wide range of coupling strengths. Under suitable conditions, CROT gates are also expected to be well protected from charge and gate noise [26]. These gates can tolerate over 2 orders of magnitude of variability in  $J$ , which means that atomically precise donor placement is not required. The two-qubit gates described here can be applied locally, in separate interaction regions. Spin transport, possibly via coherent tunnelling by adiabatic passage (CTAP) rails [27] or spin buses [28], as in the framework proposed by Hollenberg *et al.* [14], could be utilized to implement a scalable quantum computing architecture.

## II. PROPOSED SYSTEM AND THEORETICAL REPRESENTATION

We consider a system of two donors in which each electron spin represents a single qubit, with basis states  $|\downarrow\rangle$  and  $|\uparrow\rangle$ . We assume the donors are placed in a large external magnetic field  $B_0 = 1$  T, causing an energy splitting of the single-electron qubit states  $\gamma_e B_0 \approx 28$  GHz, where  $\gamma_e$  is the electron-spin gyromagnetic ratio. For the coupled two-qubit system, the computational basis is  $|\uparrow\uparrow\rangle, |\uparrow\downarrow\rangle, |\downarrow\uparrow\rangle$  and  $|\downarrow\downarrow\rangle$ . Including the nuclear spins, the Hamiltonian becomes (in units of frequency)

$$H = \gamma_e B_0 (S_{1z} + S_{2z}) + \gamma_n B_0 (I_{1z} + I_{2z}) + A_1 (\mathbf{S}_1 \cdot \mathbf{I}_1) + A_2 (\mathbf{S}_2 \cdot \mathbf{I}_2) + J (\mathbf{S}_1 \cdot \mathbf{S}_2), \quad (1)$$

where the subscript 1 (or 2) refers to donor 1 (or 2),  $\gamma_n$  is the nuclear gyromagnetic ratio,  $\mathbf{S}$  (or  $\mathbf{I}$ ) is the electron (or nuclear) spin operator with the  $z$  component  $S_z$  (or  $I_z$ ), and  $A$  is the hyperfine interaction. In the following, we will focus on a pair of  $^{31}\text{P}$  donors in silicon, but our conclusions are also valid for other donor species in silicon. We allow for different values of  $A$  in the two donors since the

different local electric fields can Stark shift the hyperfine coupling [29]. We define  $\Delta A = (A_2 - A_1)/2$  and  $\bar{A} = (A_1 + A_2)/2$ . The bulk value for  $A$  for  $^{31}\text{P}$  donors is 117 MHz, and we assume  $|\Delta A|/\bar{A}$  to be in the range of 1%–4%, i.e.,  $\Delta A \sim$  a few MHz, as expected for  $^{31}\text{P}$  donors spaced by about 20 nm in a similar nanostructure [30]. The parameters  $J, A_1, A_2$  depend on local electric fields and the exact positions of the two donors, and they can be extracted from an experiment that we describe in Sec. V.

The coupled donor-pair spin Hamiltonian has been studied by Refs. [31–35] in a high magnetic field where  $\gamma_e B_0 \gg J$  and  $\bar{A}$ . At high fields, where  $(\gamma_e - \gamma_n) B_0 \gg \bar{A}$ , the electrons and nuclei are sufficiently detuned from hyperfine mixing such that their eigenstates can mostly be treated separately. The effect of the relative strengths of  $J$  and  $\bar{A}$  on the dynamics of the electrons is the foundation of the proposals in this paper.

## III. HYPERFINE-REGULATED SWAP GATES

The  $\sqrt{\text{SWAP}}$  operation between two qubits is one of the simplest entangling quantum logic gates that, combined with single-qubit rotations, can be used for universal quantum computation. Its physical implementation with single-spin qubits requires a tunable exchange interaction  $J$ . Previous donor-based qubit proposals suggested tuning  $J$  via direct modification of the tunnel barrier [4,14,36], requiring precise placement of a  $J$  gate between the coupled donors. Instead, we suggest tuning  $J$  by detuning the donor potentials by an amount  $\varepsilon = E_1^0 - E_2^0$ , where  $E^0$  is the electrochemical potential of each donor in the neutral  $D^0$  state [see Figs. 1(a) and 1(b)]. This method is widely used in double quantum dot systems in the singlet-triplet configuration [37]; however, there the “detuning” is defined as the energy difference between the (1,1) and (0,2) charge configurations. Since in our scheme each donor spin represents a qubit, we do not advocate coming too close to the (0,2) charge configuration—this would correspond to moving the donor pair from a  $(D^0, D^0)$  to a  $(D^+, D^-)$  state. Nevertheless,  $J(\varepsilon)$  can be significantly tuned [38] from its minimum value at  $\varepsilon \approx 0$  to a higher value at  $\varepsilon < E_c$ , where  $E_c \sim 35$  meV is the donor charging energy [39]. This significantly relaxes the requirements on the nanofabrication since the control gates only need to be adjacent to the donor pair.

In the first proposal of this paper, we show how SWAP operations can be switched on and off with modest control of  $J(\varepsilon)$ . A perfect  $\text{SWAP}^\alpha$  operation is a rotation of angle  $\alpha\pi$  exactly about the  $J$  axis in the  $\mathcal{S} - \mathcal{T}_0$  Bloch sphere [see Fig. 1(c)], where  $\mathcal{S} = (|\uparrow\downarrow\rangle - |\downarrow\uparrow\rangle)/\sqrt{2}$  and  $\mathcal{T}_0 = (|\uparrow\downarrow\rangle + |\downarrow\uparrow\rangle)/\sqrt{2}$ . The  $|\uparrow\uparrow\rangle, |\downarrow\downarrow\rangle$  states are unaffected by the exchange interaction and, since we always assume  $J \ll \gamma_e B_0$ , they do not enter into the problem at any stage.

Existing proposals rely on gate control of  $J$  to vary the frequency of the exchange oscillations from (ideally) zero

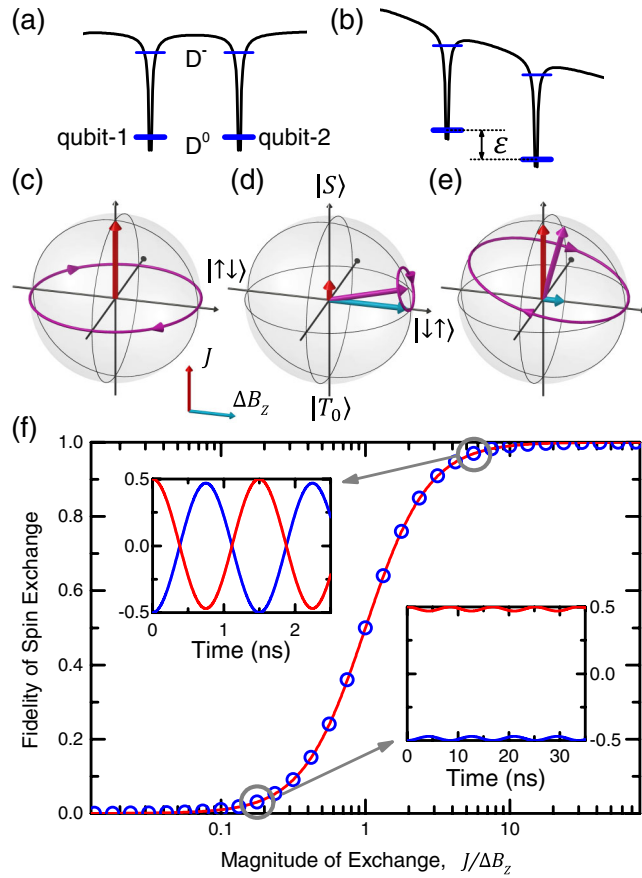


FIG. 1. (a),(b) Schematic of the conduction band profile of the coupled donor pair with qubit-1 and qubit-2 (a) in resonance and (b) detuned by  $\epsilon$ . (c)-(e) Precession on the  $S - T_0$  Bloch spheres with initial state  $|\downarrow\uparrow\rangle$  for exchange-coupled electrons (c) in the absence of coupling to nuclei, (d) where  $J < \Delta B_z$  and (e) where  $J > \Delta B_z$ . (f) Maximum fidelity of spin-state exchange between the two donor electrons as a function of  $J$  normalized to  $\Delta B_z$ . The insets show the time evolution of the expectation value of the electrons initialized as  $|\downarrow\uparrow\rangle$  for two values of  $J$ , illustrating the ability to control the amplitude of exchange oscillations.

to a maximum value  $J_{\text{on}}$ . Any residual interaction  $J_{\text{off}}$  after the  $\text{SWAP}^\alpha$  operation would result in further—unwanted—evolution of the qubits. For example, the qubit readout method based on spin-dependent tunneling requires a wait time of order  $10 \mu\text{s} - 1 \text{ms}$  between the end of the operation and the readout event [1]. Performing a  $\sqrt{\text{SWAP}}$  operation in  $10 \text{ns}$  requires  $J_{\text{on}} = 25 \text{MHz}$ , but ensuring that the resulting states have not changed by more than 1% after  $1 \text{ms}$  requires  $J_{\text{off}} < 32 \text{Hz}$ : a 6 order of magnitude dynamic range that is extremely challenging to achieve.

Our proposal focuses on controlling the amplitude of the exchange oscillations instead. We first note that the nuclear spins are also subject to a mutual coupling  $J_n$  mediated by  $A$  and  $J$  [4]. However, this coupling is very small—a few kHz even for  $J \gg 1 \text{GHz}$ , so we can assume  $J_n$  to be negligible relative to the other energy terms of the nuclear

states. Recalling that the nuclear states have negligible mixing with the electronic states in a high magnetic field, we can say that the nuclear eigenstates are, to a very good approximation, the separable  $|\uparrow\uparrow\rangle$ ,  $|\uparrow\downarrow\rangle$ ,  $|\downarrow\uparrow\rangle$ , and  $|\downarrow\downarrow\rangle$  states. The nuclei can be initialized in any of their eigenstates by adopting the single-shot readout and control techniques recently demonstrated in Ref. [3]. The initialization fidelity thus corresponds to the readout fidelity, which was  $> 99.8\%$  in Ref. [3], and has been further improved in more recent experiments [40]. Once initialized, the individual nuclei can be treated as static, such that nucleus  $i$  contributes an additional local magnetic field  $A_i/2$  or  $-A_i/2$  to its respective electron when in the  $|\uparrow\rangle$  or  $|\downarrow\rangle$  state, respectively. This results in a magnetic-field difference for the two electrons,  $\Delta B_z = |\langle\downarrow|H|\downarrow\rangle - \langle\uparrow|H|\uparrow\rangle|$ . When the nuclei are parallel ( $|\uparrow\uparrow\rangle$  or  $|\downarrow\downarrow\rangle$ ),  $\Delta B_z = \Delta A$ , and when they are antiparallel ( $|\uparrow\downarrow\rangle$  or  $|\downarrow\uparrow\rangle$ ),  $\Delta B_z = \bar{A}$ . We can, therefore, switch the strength of  $\Delta B_z$  by 1–2 orders of magnitude—in a “digital” fashion—through preparation of the nuclear states. However, dynamically switching the nuclear states requires rather long time scales (around  $10 \mu\text{s}$  for a  $\pi$  pulse and around  $100 \text{ms}$  for high-fidelity projective readout [3]). Once the nuclei have been prepared in an antiparallel state, a  $\text{SWAP}^\alpha$  operation can be implemented very rapidly by gate tuning  $J$  until it becomes larger than  $\Delta B_z$ . After a time  $\tau = \alpha/(2\sqrt{J^2 + \Delta B_z^2}) \approx \alpha/(2J)$ , the system is pulsed back to the regime  $J \ll \Delta B_z$ , where the exchange oscillations are frozen [see Fig. 1(d)], completing the  $\text{SWAP}^\alpha$  operation. For  $\Delta B_z = \bar{A} \approx 120 \text{MHz}$ , pulsing  $J$  to  $10 \times \Delta B_z$  would yield a  $\sqrt{\text{SWAP}}$  operation in  $340 \text{ps}$ .

Figure 1(f) shows calculations and simulations of the fidelity in the “on” and “off” regimes. The fidelity of spin exchange is plotted on the vertical axis and  $J/\Delta B_z$  on the horizontal axis, where  $\Delta B_z$  is  $\Delta A$  for parallel nuclei and  $\bar{A}$  for antiparallel nuclei. The insets of Fig. 1(f) show the evolution of the expectation value of the two electrons, where  $\langle S_z \rangle$  is plotted for electron 1 (blue line) and 2 (red line) initialized in the  $|\downarrow\uparrow\rangle$  state, calculated using the full Hamiltonian (1). The blue circles in Fig. 1(f) correspond to the fidelity of the oscillations in these time-evolution simulations and are calculated as  $\max(|\langle\psi|\uparrow\downarrow\rangle|^2)$ . They represent the process fidelity for a full  $\text{SWAP}$  operation. A  $\sqrt{\text{SWAP}}$  operation, which is the two-qubit entangling operation, can be obtained for any  $J/\Delta B_z > 1$  by pulsing  $J$  for the appropriate length of time. Therefore, its fidelity depends on the accuracy of the pulse calibration and the stability of the value of  $J$  during the operation. The Rabi formula for the  $S - T_0$  Bloch sphere,  $J^2/(J^2 + \Delta B_z^2)$ , follows the time-evolution calculations very closely, validating the simplified picture of the system limited to the  $S - T_0$  Bloch sphere. The results in Fig. 1(f) show that  $\text{SWAP}$  operations can be switched on and off with a fidelity of 99% by pulsing  $J$  between  $\Delta B_z/10$  and

$10\Delta B_z$ —2-orders-of-magnitude control of  $J$  is sufficient. An alternative method to perform SWAP <sup>$\alpha$</sup>  operations would be to use Euler angle construction [41], allowing for exact rotations about the  $J$  axis and further reducing the tuning capabilities required.

#### IV. CROT GATES

The CROT operation is another two-qubit gate that can be achieved with the exchange-coupled two-donor system. Importantly, our proposed realization of the operation does not require any tuning of  $J$ , further simplifying its practical implementation. In demonstrating how the system can be used to implement a CROT gate, we make some necessary approximations and quantify the associated errors.

Fidelity is most often calculated as average gate fidelity over all input states [42]. Perhaps a more meaningful quantity is the minimum fidelity considering all possible input states, though this is more difficult to calculate. We choose to provide an intuitive measure of the operator fidelity that approximates the minimum fidelity. Our method is to calculate the total fidelity  $F$  by adding, as independent events, the worst-case errors associated with each approximation we make to the Hamiltonian of the system. The worst-case fidelity for each approximation is defined as  $\min_{\psi_i} (|\langle \psi_{\text{actual}} | \psi_{\text{ideal}} \rangle|^2)$ , where  $\psi_{\text{ideal}}$  and  $\psi_{\text{actual}}$

are the output states of the operator with and without the approximation, given an input state  $\psi_i$ . The input state that yields the minimum fidelity is easy to identify for each individual approximation. The total fidelity  $F$  is then plotted in Figs. 2(c) and 2(d) as a function of  $J$  and  $T_{\text{CROT}}$ , the gate operation time. The two panels show the fidelities for two concentrations of  $^{29}\text{Si}$ , as will be explained later.

We propose to operate the CROT gate under the condition  $J < \bar{A} \ll \gamma_e B_0$ . We prepare the nuclei in either the  $|\uparrow\uparrow\rangle$  or  $|\downarrow\uparrow\rangle$  eigenstate, where they are static and do not participate in the dynamics of the electrons. The  $\Delta B_z$  experienced by the two electrons for this nuclear configuration is  $\bar{A}$ . We thus define an electron-only Hamiltonian in the computational basis with the nuclei initialized in the  $|\downarrow\uparrow\rangle$  state,

$$H_1 = \begin{bmatrix} E_{\uparrow\uparrow} & 0 & 0 & 0 \\ 0 & E_{\uparrow\downarrow} & J/2 & 0 \\ 0 & J/2 & E_{\downarrow\uparrow} & 0 \\ 0 & 0 & 0 & E_{\downarrow\downarrow} \end{bmatrix}, \quad (2)$$

where  $E_{\uparrow\uparrow} = \gamma_e B_0 + \frac{J}{4} + \frac{\Delta A}{2}$ ,  $E_{\uparrow\downarrow} = \frac{-J}{4} + \frac{\bar{A}}{2}$ ,  $E_{\downarrow\uparrow} = \frac{-J}{4} + \frac{\bar{A}}{2}$ , and  $E_{\downarrow\downarrow} = -\gamma_e B_0 + \frac{J}{4} + \frac{-\Delta A}{2}$ . We rotate away the  $J$  terms, leaving the Hamiltonian diagonalized using the change of basis matrix with the eigenstates of the Hamiltonian:  $|\widetilde{\uparrow\uparrow}\rangle$ ,  $|\widetilde{\downarrow\downarrow}\rangle$  and

$$|\widetilde{\uparrow\downarrow}\rangle = \cos\theta|\uparrow\downarrow\rangle - \sin\theta|\downarrow\uparrow\rangle, \quad (3)$$

$$|\widetilde{\downarrow\uparrow}\rangle = \cos\theta|\downarrow\uparrow\rangle + \sin\theta|\uparrow\downarrow\rangle, \quad (4)$$

where  $\tan 2\theta = J/\bar{A}$ . The corresponding eigenenergies are  $E_{\widetilde{\uparrow\downarrow}} = -J/4 - \sqrt{\bar{A}^2 + J^2}/2$  and  $E_{\widetilde{\downarrow\uparrow}} = -J/4 + \sqrt{\bar{A}^2 + J^2}/2$ .

Figure 2(a) shows a level diagram of the four eigenstates of the system including the allowed electron-spin resonance (ESR) transitions, and Fig. 2(b) shows a schematic of the corresponding ESR spectrum. We define the notation, e.g.,  $\nu_{\uparrow\downarrow}$  to be the transition frequency corresponding to rotating the second electron when the first electron is  $|\uparrow\rangle$ . We see that

$$\nu_{\uparrow\downarrow} = \gamma_e B_0 + \frac{\Delta A}{2} + \frac{J}{2} + \frac{\sqrt{\bar{A}^2 + J^2}}{2}, \quad (5)$$

$$\nu_{\downarrow\downarrow} = \gamma_e B_0 + \frac{\Delta A}{2} - \frac{J}{2} + \frac{\sqrt{\bar{A}^2 + J^2}}{2}, \quad (6)$$

$$\nu_{\downarrow\uparrow} = \gamma_e B_0 + \frac{\Delta A}{2} + \frac{J}{2} - \frac{\sqrt{\bar{A}^2 + J^2}}{2}, \quad (7)$$

$$\nu_{\uparrow\uparrow} = \gamma_e B_0 + \frac{\Delta A}{2} - \frac{J}{2} - \frac{\sqrt{\bar{A}^2 + J^2}}{2}. \quad (8)$$

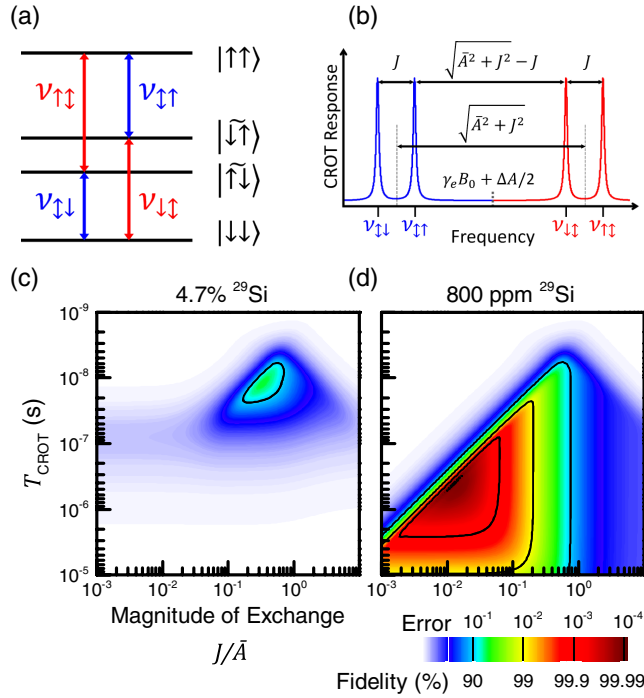


FIG. 2. (a) Schematic of the level diagram for the two-donor system with the nuclei prepared in the  $|\downarrow\uparrow\rangle$  state. (b) Schematic of the corresponding ESR spectrum. (c),(d) Contour plots of the fidelity of the proposed CROT gate as a function of  $J$  and  $T_{\text{CROT}}$ , calculated on the basis of the experimental values of the ESR line widths in (c) natural silicon and (d) isotopically purified silicon.

We define our CROT operation to be a  $\pi$  rotation at  $\nu_{\downarrow\uparrow}$ . An ideal CROT, however, would be a  $\pi$  rotation between  $|\downarrow\downarrow\rangle$  and  $|\downarrow\uparrow\rangle$ , not between  $|\downarrow\downarrow\rangle$  and  $|\downarrow\uparrow\rangle$ . Using the protocol outlined earlier for calculating the associated error, clearly  $\psi_{\text{actual}}$  and  $\psi_{\text{ideal}}$  are  $|\downarrow\uparrow\rangle$  and  $|\downarrow\uparrow\rangle$ . The inherent error introduced in the operation is  $\sin^2\theta$ . This error increases with  $J$  and is independent of  $T_{\text{CROT}}$  and the material, thus appearing as a vertical boundary in the high- $J$  region of the fidelity plots, Figs. 2(c) and 2(d).

The CROT operation is obtained by applying a magnetic field, rotating at frequency  $\nu$  in the plane perpendicular to the external magnetic field, with time-dependent amplitude  $B_1(t)$ . Transforming this perturbation into the dressed basis, the Hamiltonian in the rotating frame is

$$H_2 = \begin{bmatrix} E_{\uparrow\uparrow} - \nu & \gamma_e B_1(t) \mu_S & \gamma_e B_1(t) \mu_T & 0 \\ \gamma_e B_1(t) \mu_S & E_{\uparrow\downarrow} & 0 & \gamma_e B_1(t) \mu_S \\ \gamma_e B_1(t) \mu_T & 0 & E_{\downarrow\uparrow} & \gamma_e B_1(t) \mu_T \\ 0 & \gamma_e B_1(t) \mu_S & \gamma_e B_1(t) \mu_T & E_{\downarrow\downarrow} + \nu \end{bmatrix}, \quad (9)$$

where  $\mu_S = (\cos\theta - \sin\theta)/2$  and  $\mu_T = (\cos\theta + \sin\theta)/2$ . We now have  $\gamma_e B_1(t)$  coupling the four transitions  $\nu_{\uparrow\uparrow}$ ,  $\nu_{\downarrow\downarrow}$ ,  $\nu_{\uparrow\downarrow}$ , and  $\nu_{\downarrow\uparrow}$ , with different apparent amplitudes  $[\gamma_e B_1(t)(\cos\theta \pm \sin\theta)/2]$  depending on the states involved. Our next approximations will be to remove these coupling terms in the Hamiltonian for all off-resonant transitions. To quantify the error associated with these approximations, we treat each transition as an independent qubit system with relevant coupling and detuning and determine the transition probability due to  $\gamma_e B_1(t)$ . Nonzero probabilities at  $\nu_{\uparrow\uparrow}$ ,  $\nu_{\uparrow\downarrow}$ , and  $\nu_{\downarrow\downarrow}$  are considered errors. In addition to this, a nonunity probability at  $\nu_{\downarrow\uparrow}$  (the chosen CROT frequency) is also an error event.

We assume that the CROT gate at frequency  $\nu_{\downarrow\uparrow}$  is obtained by applying a resonant microwave pulse with a Gaussian envelope. Its excitation profile  $f_V$  [43] is many orders of magnitude more selective than that of a square pulse, especially at large detunings. Other shapes with similar selectivity, such as the Hermite pulse, are also possible candidates [42] for the CROT gate. The excitation amplitude we choose is defined as

$$B_1(t) = B_1^{\text{max}} \exp\left(-\frac{(t - T_{\text{CROT}}/2)^2}{2(T_{\text{CROT}}/6)^2}\right), \quad t \in [0, T_{\text{CROT}}], \quad (10)$$

where the pulse length  $T_{\text{CROT}}$  is 6 times the standard deviation of the Gaussian to sufficiently approximate the function. The time  $T_{\text{CROT}}$  necessary for a  $\pi$  rotation is inversely related to  $B_1^{\text{max}}$ —the complete relationship is given in Ref. [43]. For example, to perform a  $\pi$  rotation in

100 ns,  $B_1^{\text{max}}$  would need to be 0.43 mT for a Gaussian pulse and 0.18 mT for a square pulse. We also take into account the modification of the apparent amplitude of  $B_1$  depending on the states involved,  $\mu(\theta)$ . We define the probability that a  $\pi$  rotation occurs for a certain transition, with frequency  $\nu_i$  and corresponding  $\mu(\theta)$ , as

$$p_\pi = \int_{-\infty}^{\infty} f_V(\nu_{\downarrow\uparrow}, T_{\text{CROT}}, \mu(\theta), \nu) P(\nu_i, \sigma, \nu) d\nu. \quad (11)$$

Here,  $P(\nu_i, \sigma, \nu)$  describes the broadening of the resonance, a normalized Gaussian distribution with standard deviation  $\sigma$ , centered at  $\nu_i$  [2]. The first source of broadening is the fluctuation in the surrounding bath of  $^{29}\text{Si}$  spins [44]. As the contribution to the broadening depends on the  $^{29}\text{Si}$  concentration, we calculate  $F$  for qubits in natural silicon ( $^{\text{nat}}\text{Si}$ ), which contains 4.7% spin-carrying  $^{29}\text{Si}$  nuclei [see Fig. 2(c)], and in isotopically purified  $^{28}\text{Si}$  with 800 ppm residual  $^{29}\text{Si}$  atoms ( $^{\text{iso}}\text{Si}$ ) [see Fig. 2(d)]. The other possible source of broadening is the modulation of  $A$ ,  $\gamma_e$ , or  $J$  due to coupling to electric-field noise. We use the line widths obtained from ESR data on single  $^{31}\text{P}$  donors in gated silicon nanostructures,  $\sigma = 3.2$  MHz for  $^{\text{nat}}\text{Si}$  [2] and  $\sigma = 2$  kHz for  $^{\text{iso}}\text{Si}$  [40]. These experimental values inherently include broadening due to the spin bath, and the modulation of  $A$  and  $\gamma_e$  via electric-field noise, but not of  $J$ . The effect on  $J$  is difficult to predict, and we neglect it here.

Looking at the fidelity plots, we can see the error associated with the partial excitation (nonzero  $p_\pi$ ) of off-resonant transitions. The diagonal fidelity boundary at the top left is due to the proximity of  $\nu_{\uparrow\uparrow}$  to  $\nu_{\downarrow\downarrow}$ . Faster gates, corresponding to shorter  $T_{\text{CROT}}$  and broader excitation profiles, require a higher  $J$  to separate the two resonances. The diagonal fidelity boundary at the top right is due to the  $\nu_{\uparrow\downarrow}$  coming closer to  $\nu_{\downarrow\uparrow}$  as  $J$  increases. These two boundaries appear at the same positions for both  $^{\text{nat}}\text{Si}$  and  $^{\text{iso}}\text{Si}$  since they mainly depend on the spectral separation of the lines given by  $J$  and  $\bar{A}$  which, in both cases, is larger than the quoted line widths for the inhomogeneous broadening.

The final type of error is the incomplete excitation (nonunity  $p_\pi$ ) of the CROT transition. The excitation profile must be sufficiently wide (short  $T_{\text{CROT}}$ ) as compared to the inhomogeneous broadening to successfully drive the  $\pi$  rotation at  $\nu_{\downarrow\uparrow}$ . This results in the horizontal fidelity boundary at the bottom of Figs. 2(c) and 2(d). We see that this boundary allows for longer  $T_{\text{CROT}}$  in  $^{\text{iso}}\text{Si}$  [Fig. 2(d)] as compared to  $^{\text{nat}}\text{Si}$  [Fig. 2(c)], effectively “unveiling” a large region of high fidelities. In natural silicon, fidelities of about 95% are achievable for a range of  $J$  values over almost an order of magnitude, with gate times around 30 ns. In the isotopically purified material, the peak fidelity achievable exceeds 99.99%, with a gate time of 400 ns. Fidelities greater than 99.9% are achievable for a range of  $J$  values over around 1.5 orders of magnitude, with gate times

as short as 80 ns. From a practical perspective, the important result is that fidelities greater than 99% are achievable for a range of  $J$  values varying over about 2.6 orders of magnitude. This means that even fabrication methods such as ion implantation [45–47], which inherently suffer from imprecisions in the donor placement, become realistically suitable for multiqubit donor structures. Also, a recent proposal shows that donor pairs can be exchange coupled via an intermediate multielectron quantum dot [48]. The typical coupling strengths  $J \sim 100$  kHz in that proposal would yield about 99.9% fidelity for the CROT gates in <sup>iso</sup>Si described here. Given the demonstrated ability to fabricate top-gated few-electron quantum dots in silicon [49] that can be tunnel coupled to donors [1], donor-dot hybrids could constitute an appealing new strategy for fabrication and scaleup.

Having quantified the errors associated with applying the excitation, we can make the secular approximation to the Hamiltonian with  $\nu = \nu_{\downarrow\uparrow} = E_{\downarrow\uparrow}^{\sim} - E_{\downarrow\downarrow}$ ,

$$H_3 = \begin{bmatrix} E_{\uparrow\uparrow} - (E_{\downarrow\uparrow}^{\sim} - E_{\downarrow\downarrow}) & 0 & 0 & 0 \\ 0 & E_{\downarrow\uparrow}^{\sim} & 0 & 0 \\ 0 & 0 & E_{\downarrow\uparrow}^{\sim} & \gamma_e B_1(t) \mu_T \\ 0 & 0 & \gamma_e B_1(t) \mu_T & E_{\downarrow\uparrow}^{\sim} \end{bmatrix}. \quad (12)$$

The Hamiltonian above is suitable to perform a conditional rotation, where the errors arising from the three approximations have been summed to provide a conservative estimate of the overall fidelity. The resulting gate rotates the spin by an angle  $2\phi = \int 2\pi\gamma_e B_1(t)(\cos\theta + \sin\theta)dt$  within time  $t$ , described by the time-evolution operator

$$U(t) = \begin{bmatrix} e^{i\gamma_1} & 0 & 0 & 0 \\ 0 & e^{i\gamma_2} & 0 & 0 \\ 0 & 0 & e^{i\gamma_3} \cos\phi & -ie^{i\gamma_3} \sin\phi \\ 0 & 0 & -ie^{i\gamma_3} \sin\phi & e^{i\gamma_3} \cos\phi \end{bmatrix}, \quad (13)$$

where we have made the substitutions  $\gamma_1 = -t(E_{\uparrow\uparrow} - (E_{\downarrow\uparrow}^{\sim} - E_{\downarrow\downarrow}))$ ,  $\gamma_2 = -t(E_{\downarrow\uparrow}^{\sim})$ , and  $\gamma_3 = -t(E_{\downarrow\uparrow}^{\sim})$  for compactness. A single pulse of the above operator with  $U(t: 2\phi = \pi)$  yields an operation that closely resembles the CROT,

$$U_2 = \begin{bmatrix} e^{i\gamma_1} & 0 & 0 & 0 \\ 0 & e^{i\gamma_2} & 0 & 0 \\ 0 & 0 & 0 & -ie^{i\gamma_3} \\ 0 & 0 & -ie^{i\gamma_3} & 0 \end{bmatrix}. \quad (14)$$

The above operation successfully rotates the spin of the second electron conditional upon the state of the first. In order to complete the CROT (or CNOT) operation, however, the resulting phases must be accounted for. The operator causes a phase shift for each of the four basis states  $(\theta_{\uparrow\downarrow}, \theta_{\downarrow\uparrow}, \theta_{\uparrow\uparrow}, \theta_{\downarrow\downarrow})$ , which can be easily extracted by taking the phase of the nonzero element in the associated column for each basis state. It is useful to analyze, instead, the phases associated with electron 1 ( $\theta_1$ ) and electron 2 ( $\theta_2$ ), the phase due to the interaction ( $\theta_{12}$ ), and the global phase ( $\theta_g$ ). Only  $\theta_1$ ,  $\theta_2$ , and  $\theta_g$  can be corrected for with single-qubit rotations, requiring that our CROT have  $\theta_{12} = 0$ . For the above operator,  $\theta_{12} = \frac{1}{4}(\theta_{\uparrow\downarrow} + \theta_{\downarrow\uparrow} - \theta_{\uparrow\uparrow} - \theta_{\downarrow\downarrow}) = \frac{1}{4}(\gamma_2 - \gamma_1)$ . One possible solution is to use a refocusing pulse to correct for this phase as follows:

$$U_3 = X_2 U_{\sqrt{\text{CROT}}} X_2 U_{\sqrt{\text{CROT}}}, \quad (15)$$

where  $U_{\sqrt{\text{CROT}}}$  is  $U(t: 2\phi = \pi/2)$  and  $X_2$  unconditionally flips the spin of the second (target) electron. For the phase to be refocused,  $X_2$  must have  $\theta_{12} = 0$ . The two transitions  $\nu_{\uparrow\downarrow}$  and  $\nu_{\downarrow\uparrow}$  must both undergo a  $\pi$  rotation in the same amount of time. This is satisfied by the operator

$$X_2 = \begin{bmatrix} 0 & -ie^{i\gamma_2} & 0 & 0 \\ -ie^{i\gamma_2} & 0 & 0 & 0 \\ 0 & 0 & 0 & -ie^{i\gamma_3} \\ 0 & 0 & -ie^{i\gamma_3} & 0 \end{bmatrix}, \quad (16)$$

where  $\theta_{12} = 0$ . This may be implemented as a two-tone pulse with amplitude adjusted for the  $(\cos\theta + \sin\theta)$  difference in the transition matrix elements between the two pairs of states. The result of Eq. (15) yields the full operator for the CROT, which successfully completes a conditional rotation and cancels out the phase due to the interaction.

In the analysis above, we have made a realistic estimate of the CROT gate errors that could arise from fluctuations of the qubits' resonance frequencies due to random hyperfine couplings to the surrounding <sup>29</sup>Si bath. Once an exchange interaction  $J$  acts in the two-qubit Hamiltonian, electrical noise from switching charges and gate voltage fluctuations [26] can introduce further shifts of the instantaneous operation frequencies and therefore constitute an additional source of error. Here, we do not attempt to estimate the magnitude of such errors, but we note that our CROT scheme can be implemented while the two donors are at the same electrochemical potential,  $\varepsilon = 0$ . A thorough noise analysis of exchange-coupled singlet-triplet qubits has

unambiguously shown that the dephasing time  $T_2^*$  is inversely proportional to  $dJ/d\varepsilon$ , whereas no effects of charge or gate noise on the tunnel barrier height could be observed [50]. Since  $J$  is at a minimum when  $\varepsilon = 0$  [38] and  $dJ/d\varepsilon = 0$  under that circumstance [51–53], CROT operations can be performed while the coupled two-qubit system is, to first order, immune to fluctuations in  $\varepsilon$ . In this context, the lateral gates could be used to tune the system to the  $dJ/d\varepsilon = 0$  condition, even in the presence of static local disorder [54].

## V. ESR SPECTRUM

The exchange coupling  $J$  between the two donors in each interaction region needs to be calibrated in order to perform either of the proposed two-qubit logic gates. Given a Hamiltonian  $H(J)$ ,  $J$  can be extracted from the ESR spectrum obtained by performing an experiment similar to that of Ref. [2]. This “ESR fingerprint” (see Fig. 3) is calculated by considering all transitions between the eigenstates of  $H(J)$  in the regime  $J < \gamma_e B_0$ . Their respective intensities are weighted with (i) the electronic transition dipole matrix elements,  $\langle \psi_i | (\sigma_{x_{S1}} + \sigma_{x_{S2}}) | \psi_f \rangle$ , where  $\sigma_{x_{S_n}}$  is the Pauli operator for electron  $n$ , and (ii) the readout contrast, i.e., the change in expectation value of the spin- $z$  projection of each electron upon excitation of the ESR transition,  $\Delta \langle S_{n_z} \rangle = \langle \psi_f | S_{n_z} | \psi_f \rangle - \langle \psi_i | S_{n_z} | \psi_i \rangle$ . The

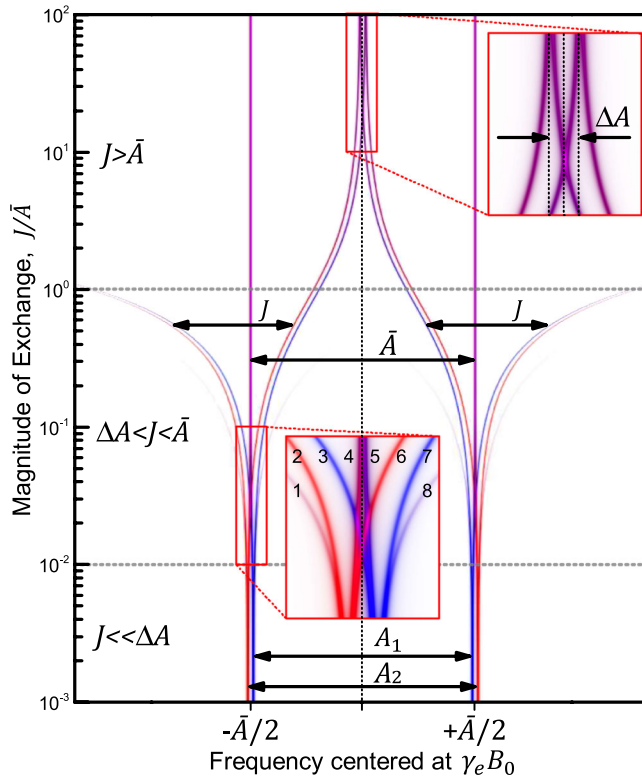


FIG. 3. The ESR fingerprint of  $H(J)$  plotted as a function of the exchange-hyperfine interaction ratio. Branches are labeled from left to right (1 to 16) on the  $J = 10^{-1} \bar{A}$  line, with 1 to 8 shown.

transitions in Fig. 3 are color-coded such that the blue and red intensities are proportional to  $\Delta \langle S_{1_z} \rangle$  and  $\Delta \langle S_{2_z} \rangle$ , respectively. In the example of an allowed electronic transition,  $|\downarrow\downarrow\rangle \rightarrow |T_0\rangle$ , the line is drawn in purple since it has equal, nonzero contributions from both  $\Delta \langle S_{1_z} \rangle$  and  $\Delta \langle S_{2_z} \rangle$ . We plot in Fig. 3 an example where  $A_2 > A_1$  and  $\Delta A/\bar{A} = 2.5\%$ . The line width is taken to be smaller than  $\Delta A$  such that this splitting can be resolved.

In the  $J \ll \Delta A$  region, where the eigenstates are simply the combinations of logical electronic and nuclear states, we see a pair of blue and red lines that correspond to rotations of electron 1 and 2, respectively. The transitions at  $\gamma_e B_0 - A_i/2$  and  $\gamma_e B_0 + A_i/2$  rotate electron  $i$  when its binding nucleus is in the  $|\downarrow\rangle$  or  $|\uparrow\rangle$  state, respectively. Thus, the red line at  $\gamma_e B_0 - A_2/2$  includes the following four transitions:  $|\downarrow\downarrow\downarrow\downarrow\rangle \rightarrow |\uparrow\downarrow\downarrow\downarrow\rangle$  (branch 1),  $|\uparrow\downarrow\downarrow\downarrow\rangle \rightarrow |\uparrow\uparrow\downarrow\downarrow\rangle$  (branch 4),  $|\downarrow\downarrow\uparrow\uparrow\rangle \rightarrow |\downarrow\uparrow\uparrow\uparrow\rangle$  (branch 2), and  $|\uparrow\downarrow\uparrow\uparrow\rangle \rightarrow |\uparrow\uparrow\uparrow\uparrow\rangle$  (branch 6). In the following, we will focus our description of the transitions to the red branches on the left-hand side of the spectrum, noting that the same reasoning can directly be transferred to the other branches.

As  $J$  becomes larger than the line width (region  $J < \bar{A}$ ), we observe the exchange splitting between transitions  $|\downarrow\downarrow\downarrow\downarrow\rangle \rightarrow |\downarrow\uparrow\downarrow\downarrow\rangle$  (branch 1) and  $|\uparrow\downarrow\downarrow\downarrow\rangle \rightarrow |\uparrow\uparrow\downarrow\downarrow\rangle$  (branch 4) and between transitions  $|\downarrow\downarrow\uparrow\uparrow\rangle \rightarrow |\downarrow\uparrow\uparrow\uparrow\rangle$  (branch 2) and  $|\uparrow\downarrow\uparrow\uparrow\rangle \rightarrow |\uparrow\uparrow\uparrow\uparrow\rangle$  (branch 6). The electronic  $|\uparrow\downarrow\rangle$  and  $|\downarrow\uparrow\rangle$  states tend towards either the  $|T_0\rangle$  or  $|S\rangle$  state as  $J/\Delta B_z$  increases for each particular nuclear configuration. Branches 1 and 2 fade away for  $J \sim \Delta A$  and  $J \sim \bar{A}$ , respectively, as they involve the state approaching a magnetically inaccessible singlet state. Their  $J$ -split counterparts, branches 4 and 6, involving states approaching  $|T_0\rangle$ , tend towards  $\gamma_e B_0 - \bar{A}/2$  and  $\gamma_e B_0 - \Delta A/2$  (region  $J > \bar{A}$ ), respectively.

A transition involving a fully entangled state would have  $\Delta \langle S_{1_z} \rangle = \Delta \langle S_{2_z} \rangle = 0.5$ . Accordingly, the region where the branches become purple indicate where a participating state tends towards the  $|T_0\rangle$  or  $|S\rangle$ .

With the ability to independently prepare and read the electron state of each donor, it would be possible to observe every transition for a given  $H(J)$ . The protocol would involve preparing or, at least, randomizing the nuclear spins using appropriate nuclear magnetic resonance (NMR) pulses and then extracting the ESR spectrum for both electrons as in Ref. [2]. For a proof-of-principle device, we make the conservative assumption that only donor 2 is tunnel coupled to a charge reservoir so that its electron spin can be read out in single shot and initialized electrically in the ground state [1]. In this case, performing ESR experiments would only reveal those transitions involving  $|\downarrow\downarrow\rangle$  with  $\Delta \langle S_{2_z} \rangle > 0$ . In the  $J \lesssim \Delta A$  regime, branches 1, 2, 11, and 13 could be observed. In the  $\Delta A \lesssim J \lesssim \bar{A}$  regime, branch 1 fades away and branch 5 emerges as its  $\Delta \langle S_{2_z} \rangle$  increases. Finally, in the  $J \gtrsim \bar{A}$ , branch 2 fades away while

branch 10 emerges. The relative spacing between the lines should make it easy to extract the value of  $J$ . To be certain, slightly modifying  $J$  by shifting the electrostatic environment will allow comparison to the fingerprint in Fig. 3, ensuring a correct interpretation of the observed resonances. Operating in the  $\gamma_e B_0 \gg \bar{A}$  regime, the resonant frequencies of these transitions are determined by four parameters ( $\gamma_e B_0$ ,  $\bar{A}$ ,  $\Delta A$ , and  $J$ ) so that the determination of four resonant frequencies is sufficient to extract these parameters.

## VI. SUMMARY AND OUTLOOK

We have analyzed the system of two exchange-coupled donor-spin qubits and shown how we can harness the hyperfine interaction with the  $^{31}\text{P}$  donor nuclei to implement two different types of two-qubit logic gates that form a universal set of operations when combined with single-qubit rotations. In the first method, we show that the amplitude of exchange oscillations can be controlled by exploiting the presence of the magnetic detuning,  $\Delta B_z$ , provided by the hyperfine interaction with the donor nuclei. These oscillations can be switched on and off to form a  $\sqrt{\text{SWAP}}$  gate of 99% fidelity upon tuning  $J$  by just 2 orders of magnitude. In the second method, a two-qubit gate is implemented as the resonant rotation of one electron conditional upon the spin state of the other. This method has the significant advantage that  $J$  does not need to be tuned and a wide range of coupling strengths yields high-fidelity CROT gates in natural silicon ( $> 95\%$ ) and in isotopically purified silicon ( $> 99.99\%$ ). The CROT gate can be operated at zero electrostatic detuning, which renders the system minimally susceptible to charge noise. Additionally, the gate does not trigger the fast triplet-singlet relaxation predicted [23] and observed [24] in the presence of the interplay between strong  $J$  and a hyperfine coupling  $A$ . When  $J \sim A$ , the long single-spin lifetimes ( $T_1 \gg 1$  s) [1] can be recovered. Compared to previous proposals, our methods greatly relax the requirements on the accuracy of donor positioning and alignment of nanofabricated gates. We expect that this will facilitate the construction of donor-based quantum-information processors using ion implantation [46,47], scanning-probe lithography [55], or hybrid donor-dot devices [48]. Quantum-dot-only implementations of both the gates we described are also possible, provided the electrons in the coupled dots have individual Zeeman splittings that differ by more than the ESR line width. Large  $\Delta B_z$  values can be obtained using field gradients produced by micromagnets [18,19]. Another promising route is the use of gate-defined quantum dots on isotopically purified  $^{28}\text{Si}$ , where the  $g$  factor can be controlled by electric fields and the ESR frequency shifted by 3 orders of magnitude more than the line width [56]. We expect that the robust two-qubit logic gates described here will provide further momentum to the quest for scaling up spin-based quantum computers in semiconductors.

## ACKNOWLEDGMENTS

The authors thank F. A. Mohiyaddin, J. J. Pla, L. C. L. Hollenberg, and A. S. Dzurak for useful discussions. This research was funded by the Australian Research Council Centre of Excellence for Quantum Computation and Communication Technology (Project No. CE11E0096) and the US Army Research Office (W911NF-13-1-0024). R. K. and A. L. contributed equally to this work.

- [1] A. Morello, J. J. Pla, F. A. Zwanenburg, K. W. Chan, K. Y. Tan, H. Huebl, M. Mottonen, C. D. Nugroho, C. Yang, J. A. van Donkelaar, A. D. C. Alves, D. N. Jamieson, C. C. Escott, L. C. L. Hollenberg, R. G. Clark, and A. S. Dzurak, *Single-Shot Readout of an Electron Spin in Silicon*, *Nature (London)* **467**, 687 (2010).
- [2] J. J. Pla, K. Y. Tan, J. P. Dehollain, W. H. Lim, J. J. L. Morton, D. N. Jamieson, A. S. Dzurak, and A. Morello, *A Single-Atom Electron Spin Qubit in Silicon*, *Nature (London)* **489**, 541 (2012).
- [3] J. J. Pla, K. Y. Tan, J. P. Dehollain, W. H. Lim, J. J. L. Morton, F. A. Zwanenburg, D. N. Jamieson, A. S. Dzurak, and A. Morello, *High-Fidelity Readout and Control of a Nuclear Spin Qubit in Silicon*, *Nature (London)* **496**, 334 (2013).
- [4] B. E. Kane, *A Silicon-Based Nuclear Spin Quantum Computer*, *Nature (London)* **393**, 133 (1998).
- [5] D. D. Awschalom, L. C. Bassett, A. S. Dzurak, E. L. Hu, and J. R. Petta, *Quantum Spintronics: Engineering and Manipulating Atom-like Spins in Semiconductors*, *Science* **339**, 1174 (2013).
- [6] D. P. DiVincenzo, *Two-Bit Gates Are Universal for Quantum Computation*, *Phys. Rev. A* **51**, 1015 (1995).
- [7] J. O'Brien, G. Pryde, A. White, T. Ralph, and D. Branning, *Demonstration of an All-Optical Quantum Controlled-NOT Gate*, *Nature (London)* **426**, 264 (2003).
- [8] J. H. Plantenberg, P. C. de Groot, C. J. P. M. Harmans, and J. E. Mooij, *Demonstration of Controlled-NOT Quantum Gates on a Pair of Superconducting Quantum Bits*, *Nature (London)* **447**, 836 (2007).
- [9] K. Nowack, M. Shafiei, M. Laforest, G. Prawiroatmodjo, L. Schreiber, C. Reichl, W. Wegscheider, and L. Vandersypen, *Single-Shot Correlations and Two-Qubit Gate of Solid-State Spins*, *Science* **333**, 1269 (2011).
- [10] M. D. Shulman, O. E. Dial, S. P. Harvey, H. Bluhm, V. Umansky, and A. Yacoby, *Demonstration of Entanglement of Electrostatically Coupled Singlet-Triplet Qubits*, *Science* **336**, 202 (2012).
- [11] C. Monroe and J. Kim, *Scaling the Ion Trap Quantum Processor*, *Science* **339**, 1164 (2013).
- [12] P. Neumann, R. Kolesov, B. Naydenov, J. Beck, F. Rempp, M. Steiner, V. Jacques, G. Balasubramanian, M. Markham, D. Twitchen, S. Pezzagna, J. Meijer, J. Twamley, F. Jelezko, and J. Wrachtrup, *Quantum Register Based on Coupled Electron Spins in a Room-Temperature Solid*, *Nat. Phys.* **6**, 249 (2010).
- [13] C. D. Hill, L. C. L. Hollenberg, A. G. Fowler, C. J. Wellard, A. D. Greentree, and H.-S. Goan, *Global Control and Fast*

- Solid-State Donor Electron Spin Quantum Computing*, *Phys. Rev. B* **72**, 045350 (2005).
- [14] L. Hollenberg, A. Greentree, A. Fowler, and C. Wellard, *Two-Dimensional Architectures for Donor-Based Quantum Computing*, *Phys. Rev. B* **74**, 045311 (2006).
- [15] C. Hill, *Robust Controlled-NOT Gates from Almost Any Interaction*, *Phys. Rev. Lett.* **98**, 180501 (2007).
- [16] B. Koiller, X. Hu, and S. Das Sarma, *Strain Effects on Silicon Donor Exchange: Quantum Computer Architecture Considerations*, *Phys. Rev. B* **66**, 115201 (2002).
- [17] C. J. Wellard, L. C. L. Hollenberg, F. Parisoli, L. M. Kettle, H.-S. Goan, J. A. L. McIntosh, and D. N. Jamieson, *Electron Exchange Coupling for Single-Donor Solid-State Spin Qubits*, *Phys. Rev. B* **68**, 195209 (2003).
- [18] T. Meunier, V. E. Calado, and L. M. K. Vandersypen, *Efficient Controlled-Phase Gate for Single-Spin Qubits in Quantum Dots*, *Phys. Rev. B* **83**, 121403 (2011).
- [19] M. Pioro-Ladrière, T. Obata, Y. Tokura, Y.-S. Shin, T. Kubo, K. Yoshida, T. Taniyama, and S. Tarucha, *Electrically Driven Single-Electron Spin Resonance in a Slanting Zeeman Field*, *Nat. Phys.* **4**, 776 (2008).
- [20] F. Luis, A. Repollés, M. J. Martínez-Pérez, D. Aguilà, O. Roubeau, D. Zueco, P. J. Alonso, M. Evangelisti, A. Camón, J. Sesé, L. A. Barrios, and G. Aromí, *Molecular Prototypes for Spin-Based CNOT and Swap Quantum Gates*, *Phys. Rev. Lett.* **107**, 117203 (2011).
- [21] S. Foletti, H. Bluhm, D. Mahalu, V. Umansky, and A. Yacoby, *Universal Quantum Control of Two-Electron Spin Quantum Bits Using Dynamic Nuclear Polarization*, *Nat. Phys.* **5**, 903 (2009).
- [22] F. Beaudoin and W. A. Coish, *Enhanced Hyperfine-Induced Spin Dephasing in a Magnetic-Field Gradient*, *Phys. Rev. B* **88**, 085320 (2013).
- [23] M. Borhani and X. Hu, *Two-Spin Relaxation of p Dimers in Silicon*, *Phys. Rev. B* **82**, 241302 (2010).
- [24] J. P. Dehollain, J. T. Muhonen, K. Y. Tan, A. Saraiva, D. N. Jamieson, A. S. Dzurak, and A. Morello, *Single-Shot Readout and Relaxation of Singlet/Triplet States in Exchange-Coupled 3IP Electron Spins in Silicon*, arXiv:1402.7148.
- [25] F. Jelezko, T. Gaebel, I. Popa, M. Domhan, A. Gruber, and J. Wrachtrup, *Observation of Coherent Oscillation of a Single Nuclear Spin and Realization of a Two-Qubit Conditional Quantum Gate*, *Phys. Rev. Lett.* **93**, 130501 (2004).
- [26] D. Culcer, X. Hu, and S. Das Sarma, *Dephasing of Si Spin Qubits Due to Charge Noise*, *Appl. Phys. Lett.* **95**, 073102 (2009).
- [27] A. Greentree, J. Cole, A. Hamilton, and L. Hollenberg, *Coherent Electronic Transfer in Quantum Dot Systems Using Adiabatic Passage*, *Phys. Rev. B* **70**, 235317 (2004).
- [28] M. Friesen, A. Biswas, X. Hu, and D. Lidar, *Efficient Multiqubit Entanglement via a Spin Bus*, *Phys. Rev. Lett.* **98**, 230503 (2007).
- [29] R. Rahman, C. J. Wellard, F. R. Bradbury, M. Prada, J. H. Cole, G. Klimeck, and L. C. L. Hollenberg, *High Precision Quantum Control of Single Donor Spins in Silicon*, *Phys. Rev. Lett.* **99**, 036403 (2007).
- [30] F. A. Mohiyaddin, R. Rahman, R. Kalra, G. Klimeck, L. C. L. Hollenberg, J. J. Pla, A. S. Dzurak, and A. Morello, *Noninvasive Spatial Metrology of Single-Atom Devices*, *Nano Lett.* **13**, 1903 (2013).
- [31] C. P. Slichter, *Spin Resonance of Impurity Atoms in Silicon*, *Phys. Rev.* **99**, 479 (1955).
- [32] D. Jérôme and J. M. Winter, *Electron Spin Resonance on Interacting Donors in Silicon*, *Phys. Rev.* **134**, A1001 (1964).
- [33] J. Marko, *Broad Saturation Effect and the Background EPR Line in Phosphorus-Doped Silicon*, *Phys. Lett.* **27A**, 119 (1968).
- [34] T. Shimizu, *ESR Spectra of Donor Clusters*, *J. Phys. Soc. Jpn.* **25**, 1021 (1968).
- [35] J. H. Pifer, *Spin Delocalization in Phosphorus Donor Pairs in Silicon*, *Phys. Rev. B* **32**, 7091 (1985).
- [36] C. Wellard, L. Hollenberg, F. Parisoli, L. Kettle, H.-S. Goan, J. McIntosh, and D. Jamieson, *Electron Exchange Coupling for Single-Donor Solid-State Spin Qubits*, *Phys. Rev. B* **68**, 1 (2003).
- [37] J. R. Petta, A. C. Johnson, J. M. Taylor, E. A. Laird, A. Yacoby, M. D. Lukin, C. M. Marcus, M. P. Hanson, and A. C. Gossard, *Coherent Manipulation of Coupled Electron Spins in Semiconductor Quantum Dots*, *Science* **309**, 2180 (2005).
- [38] G. Burkard, D. Loss, and D. P. Divincenzo, *Coupled Quantum Dots as Quantum Gates*, *Phys. Rev. B* **59**, 2070 (1999).
- [39] K. Y. Tan, K. W. Chan, M. Möttönen, A. Morello, C. Yang, J. van Donkelaar, A. Alves, J.-M. Pirkkalainen, D. N. Jamieson, R. G. Clark, and A. S. Dzurak, *Transport Spectroscopy of Single Phosphorus Donors in a Silicon Nanoscale Transistor*, *Nano Lett.* **10**, 11 (2010).
- [40] J. T. Muhonen, J. P. Dehollain, A. Laucht, F. E. Hudson, T. Sekiguchi, K. M. Itoh, D. N. Jamieson, J. C. McCallum, A. S. Dzurak, and A. Morello, *Storing Quantum Information for 30 Seconds in a Nanoelectronic Device*, arXiv:1402.7140.
- [41] R. Hanson and G. Burkard, *Universal Set of Quantum Gates for Double-Dot Spin Qubits with Fixed Interdot Coupling*, *Phys. Rev. Lett.* **98**, 050502 (2007).
- [42] L. Vandersypen and I. Chuang, *NMR Techniques for Quantum Control and Computation*, *Rev. Mod. Phys.* **76**, 1037 (2005).
- [43] G. S. Vasilev and N. V. Vitanov, *Coherent Excitation of a Two-State System by a Gaussian Field*, *Phys. Rev. A* **70**, 053407 (2004).
- [44] E. Abe, A. M. Tyryshkin, S. Tojo, J. J. Morton, W. M. Witzel, A. Fujimoto, J. W. Ager, E. E. Haller, J. Isoya, S. A. Lyon *et al.*, *Electron Spin Coherence of Phosphorus Donors in Silicon: Effect of Environmental Nuclei*, *Phys. Rev. B* **82**, 121201 (2010).
- [45] D. N. Jamieson, C. Yang, T. Hopf, S. M. Hearne, C. I. Pakes, S. Praver, M. Mitic, E. Gauja, S. E. Andresen, F. E. Hudson, A. S. Dzurak, and R. G. Clark, *Controlled Shallow Single-Ion Implantation in Silicon Using an Active Substrate for Sub-20-keV Ions*, *Appl. Phys. Lett.* **86**, 202101 (2005).
- [46] A. Persaud, S. Park, J. Liddle, T. Schenkel, J. Bokor, and I. Rangelow, *Integration of Scanning Probes and Ion Beams*, *Nano Lett.* **5**, 1087 (2005).
- [47] A. Alves, J. Newnham, J. van Donkelaar, S. Rubanov, J. McCallum, and D. Jamieson, *Controlled Deterministic*

- Implantation by Nanostencil Lithography at the Limit of Ion-Aperture Straggling*, *Nanotechnology* **24**, 145304 (2013).
- [48] V. Srinivasa, X. Hu, and J. M. Taylor, *Tunable Spin Qubit Coupling Mediated by a Multi-electron Quantum Dot*, arXiv:1312.1711.
- [49] W. H. Lim, F. A. Zwanenburg, H. Huebl, M. Möttönen, K. W. Chan, A. Morello, and A. S. Dzurak, *Observation of the Single-Electron Regime in a Highly Tunable Silicon Quantum Dot*, *Appl. Phys. Lett.* **95**, 242102 (2009).
- [50] O. E. Dial, M. D. Shulman, S. P. Harvey, H. Bluhm, V. Umansky, and A. Yacoby, *Charge Noise Spectroscopy Using Coherent Exchange Oscillations in a Singlet-Triplet Qubit*, *Phys. Rev. Lett.* **110**, 146804 (2013).
- [51] M. Stopa and C. M. Marcus, *Magnetic Field Control of Exchange and Noise Immunity in Double Quantum Dots*, *Nano Lett.* **8**, 1778 (2008).
- [52] E. Nielsen, R. W. Young, R. P. Muller, and M. S. Carroll, *Implications of Simultaneous Requirements for Low-Noise Exchange Gates in Double Quantum Dots*, *Phys. Rev. B* **82**, 075319 (2010).
- [53] G. Ramon, *Electrically Controlled Quantum Gates for Two-Spin Qubits in Two Double Quantum Dots*, *Phys. Rev. B* **84**, 1 (2011).
- [54] R. Rahman, E. Nielsen, R. P. Muller, and M. S. Carroll, *Voltage Controlled Exchange Energies of a Two-Electron Silicon Double Quantum Dot with and without Charge Defects in the Dielectric*, *Phys. Rev. B* **85**, 125423 (2012).
- [55] S. Schofield, N. Curson, M. Simmons, F. Ruess, T. Hallam, L. Oberbeck, and R. Clark, *Atomically Precise Placement of Single Dopants in Si*, *Phys. Rev. Lett.* **91**, 136104 (2003).
- [56] M. Veldhorst, J. C. C. Hwang, C. H. Yang, A. W. Leenstra, B. de Ronde, J. P. Dehollain, J. T. Muhonen, F. Hudson, K. Itoh, A. Morello, and A. S. Dzurak, *A Gate-Addressable Quantum Dot Qubit with Fault-Tolerant Gate Fidelity* (unpublished).